

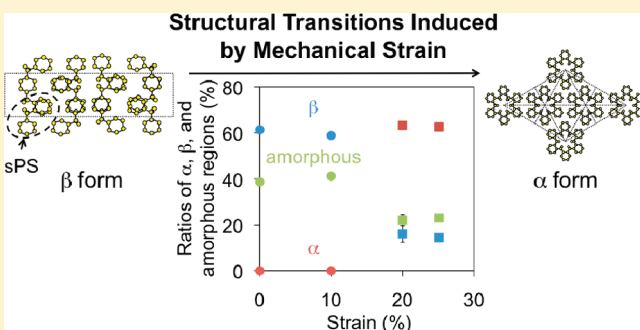
β to α Form Transition Observed in the Crystalline Structures of Syndiotactic Polystyrene (sPS)

Tetsu Ouchi, Suguru Nagasaka, and Atsushi Hotta*

Department of Mechanical Engineering, Keio University, Yokohama 223-8522, Japan

Supporting Information

ABSTRACT: A solid–solid crystalline transition from β to α forms in syndiotactic polystyrene (sPS) was found during the mechanical deformation in the temperature range of 130–218 °C, studied by X-ray and infrared spectroscopy. α and β forms, in contrast to the other two crystalline structures (γ and δ forms) in sPS, are two major crystalline forms manufactured through a concise molding process which is industrially readily accessible. There have been a number of structural transitions found between two crystalline structures among the four different crystalline forms of sPS. In this work, β to α form transition at well below the melting temperature of sPS (~ 270 °C) was found by mechanical deformation, which became more pronounced as temperature increased. The structural transition was intimately related to the crystallization temperature and the densities of α and β forms.



INTRODUCTION

sPS has been widely investigated after the first successful synthesis by Natta et al. using heterogeneous solid catalysts in 1955.¹ The low tacticity and the low purity of the sPS were then improved by Ishihara et al. in 1986, where they succeeded in producing new sPS with much higher tacticity ($[\text{rr}] = 98\%$).² Further studies on chemical and physical properties of sPS including microstructural analyses of the crystalline forms have been carried out by analyzing sPS with high tacticity in order to achieve high melting points, fast crystallization rates, high chemical and thermal resistances, and better mechanical properties.^{3–5}

The syndiotacticity of sPS induces several crystalline structures, while ordinary polystyrene (PS) without tacticity shows only amorphous features. sPS exhibits complex polymorphic behavior with four types of crystalline structures: α , β , γ , and δ (including δ_e). In more microscopic view, these crystalline structures possess different molecular conformations. α and β forms contain molecular chains in trans-planar conformations which can be obtained by melt crystallization or cold crystallization.^{3,4,6} In contrast, γ , δ , and δ_e forms contain only molecular chains in $s(2/1)2$ helical conformations which can be obtained by several solvent treatments.^{3,4,7} Because of the better mechanical properties of α and β forms possessing trans-planar conformations⁸ that can be produced through brief manufacturing processes, sPS with α and β forms are widely recognized as prospective industrial materials.

The crystalline structures of α and β forms in sPS can be obtained by various ways through the controls of temperature, melting time, cooling rate, initial crystalline forms, molecular weights, and blend compositions of polymers.^{3,4,6,9} De Rosa et al.

studied the effects of annealing temperature and melting time during molding on crystalline structures. They found that the higher annealing temperature and the longer time in melt induced β form, while on the other hand, the lower annealing temperature and the shorter melting time established α form: α form decreased and β form increased by increasing annealing temperatures from 280 to 320 °C, while α form became more dominant by shortening annealing times from 10 min to 30 s at a constant annealing temperature of 290 °C.⁶ Sun et al. reported that the sPS with lower molecular weight ($M_w = 63\,000$ g/mol) produced only β form, crystallized at the temperature range of 230–260 °C.⁹ Recently, it was found that the sPS/aPS blends made the equilibrium melting temperature lower with producing β form rather than α form.⁴ It is hence understood that α form is more kinetically stable than β form, whereas β form is more thermodynamically stable than α form.⁴ Therefore, α form can be obtained at lower temperature by faster cooling and β form can be obtained at higher temperature by slower cooling.

The detailed crystalline structures of α and β forms have been studied, and α form was found to construct a trigonal crystalline structure of $a = b = 26.26$ Å and $c = 5.04$ Å with a density of 1.03 g/cm³ in most cases.^{10,11} The density of α form is lower than that of amorphous phase (1.06 g/cm³).^{12,13} The packing model of β form is orthorhombic with $a = 8.81$ Å, $b = 28.82$ Å, and $c = 5.51$ Å,¹⁴ and the density of β form is 1.08 g/cm³, which is higher than that of α form as well as that of amorphous regions.¹⁵ The α form

Received: January 24, 2011

Revised: February 18, 2011

Published: March 11, 2011

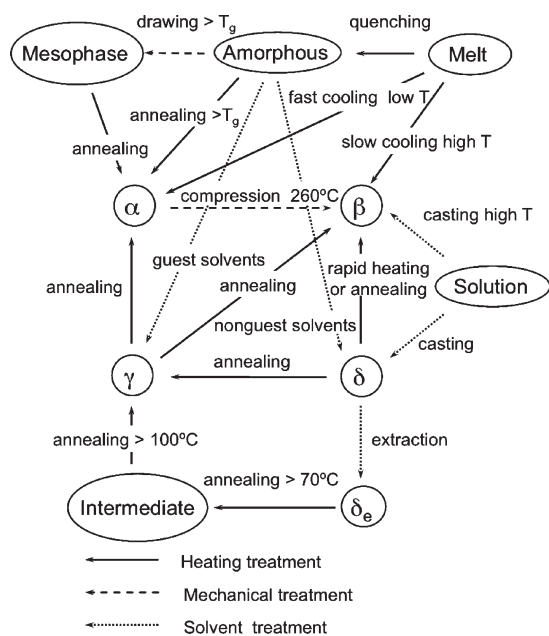


Figure 1. Schematic diagram of the crystallizations and the structural transitions of sPS.

can be further classified into limit disordered model (α') and limit ordered model (α''), while β form can be further classified into limit disordered model (β') and limit ordered model (β'').^{3,4,6} A mesomorphic α form was also reported by Auriemma et al.¹⁶ The limit models can be usually obtained by melt or cold crystallization and solution treatment, where α' is preferably produced by cold crystallization below 175 °C from amorphous sPS, and α'' can be produced at near 270 °C, which is quite close to the melting temperature of sPS.^{4,6} Similarly, β' can be formed by melt crystallization cooled from ~300 °C, while β'' form can be obtained by crystallization from solutions by rapid removal of the solution thereafter.^{3,6}

Quite a few thermal and mechanical structural transitions between the four crystalline structures (α , β , γ , and δ) have been reported, which are summarized in Figure 1.^{3,7,8,17–22} For example, Gowd et al. reported that the thermal δ to β transition occurred when δ form sample was annealed above 140 °C.¹⁹ They also found γ to α transition by annealing above 190 °C,^{3,22} and γ to β transition by annealing at temperature above 190 °C, while as for the latter transition, the transition temperature became lower with the higher amount of solvent due to the plasticizing effect of the solvent remaining in the amorphous region.^{7,19} There are no thermal transitions from (α , β) forms to (γ , δ , and δ_e) forms reported so far, which may highly be due to the thermal stability of the two α and β forms.

Just to focus on the transitions related to α and β forms, the thermal crystalline transitions between α and β forms are still controversial,^{6,23–27} while β to α transition has not been reported yet. Mechanically induced transitions, on the other hand, where the transitions were induced by external forces such as drawing and compression, were confirmed by several groups.^{8,18,28} Decandia et al. reported that amorphous to mesomorphic α transition was induced when the amorphous sample was stretched.²⁸ α to β transition induced by compression force was investigated by Sun et al., where the compression force above 118 kPa was applied to the testing sample at the high temperature of 260 °C.⁸ However, this transition should be regarded as a

quasi-solid to solid transition in the sense that, at the process temperature of 260 °C, sPS already started melting. As was mentioned above, the transition from β to α forms has not been reported yet, and in this work an actual solid to solid transition from β to α forms in sPS induced by mechanical strain at sufficiently below the melting temperature of sPS was found and reported.

EXPERIMENTS

Materials. sPS with a molecular weight of 140 000 g/mol was supplied by Idemitsu Kosan Co. Japan. Differential scanning calorimetry (DSC) analysis (DSC822, Mettler) was carried out with the heating rate of 10 °C/min from 25 to 300 °C. The glass transition temperature (T_g) was detected at around 100 °C, and the melting temperature was ~270 °C. The results from the second DSC scan were used for the analysis.

Crystallization and Molding. sPS with two types of microstructures were prepared: one type consisted of β form with an amorphous region (β specimen), and the other type consisted entirely of an amorphous phase (an amorphous specimen). β specimen was obtained by compression molding at 300 °C for 10 min followed by cooling to room temperature. An amorphous specimen was obtained by compression molding at 300 °C for 10 min followed by cold-water quenching. The microstructures of the samples were examined by X-ray scattering and X-ray diffraction analyses and Fourier-transform infrared spectroscopy (FTIR) to confirm the inner structures.

X-ray Analysis. Wide-angle X-ray scattering (WAXS) and wide-angle X-ray diffraction analysis (WAXD) (Bruker D8 Discover) were conducted to identify the microstructures of sPS before and after tensile testing using Cu K α radiation ($\lambda = 0.154$ 18 nm). The equatorial area of the X-ray profiles was scanned at the diffraction angle (2θ) ranging from 5° to 30°.^{3,29–31}

FTIR Analysis. FTIR analysis was performed using FTIR-4200 (JASCO) with infrared microspectroscopy (Irron μ IRT-1000, JASCO) to identify the crystalline structures of sPS by calculating the ratios of α , β , and amorphous regions before and after tensile testing with a wavenumber resolution of 2.0 cm⁻¹.

Spectral subtraction analysis was conducted to clearly identify the detailed microstructures of sPS, where an amorphous spectrum was subtracted from a total recorded spectrum to get an intended crystalline spectrum. α and β forms were carefully evaluated from the wavenumber of 1000 to 800 cm⁻¹ by the spectral subtraction analysis proposed by Musto et al.,³² which eliminated amorphous spectra by adjusting the 841 cm⁻¹ peak to become 0 (baseline).

To calculate the ratios of α and β , eqs 1 and 2 were used. The ratio of amorphous regions was calculated using eq 3.

$$C_{\alpha} = \frac{A_{851}/\alpha_{\alpha}}{A_{841} + A_{851}/\alpha_{\alpha} + A_{858}/\alpha_{\beta}} \times 100\% \\ = \frac{A_{851}/0.178}{A_{841} + A_{851}/0.178 + A_{858}/0.272} \times 100\% \quad (1)$$

$$C_{\beta} = \frac{A_{858}/\alpha_{\beta}}{A_{841} + A_{851}/\alpha_{\alpha} + A_{858}/\alpha_{\beta}} \times 100\% \\ = \frac{A_{858}/0.272}{A_{841} + A_{851}/0.178 + A_{858}/0.272} \times 100\% \quad (2)$$

$$100 - (C_{\alpha} + C_{\beta}) \quad (3)$$

A_{858} , A_{851} , and A_{841} represent the spectrum areas at 858, 851, and 841 cm⁻¹, respectively with an error of ± 1 cm⁻¹. α_{α} and α_{β} were

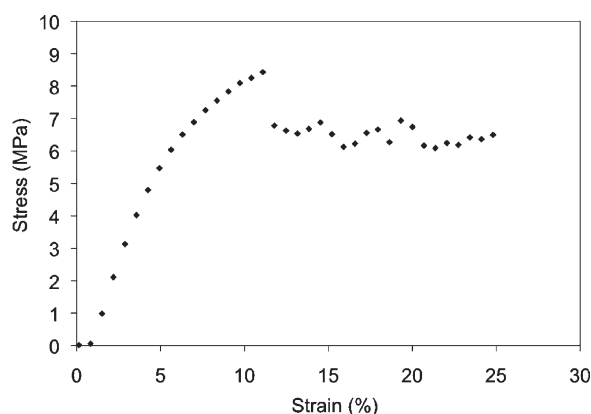


Figure 2. A stress–strain curve of β specimen at 218 °C.

indicated as 0.178 ± 0.005 and 0.272 ± 0.005 , respectively, by Wu et al.^{33–35} In this work, 0.178 and 0.272 were used for α_α and α_β to calculate C_α and C_β . Curve fitting was conducted to measure the areas of A_{858} , A_{851} , and A_{841} , referring to the wavenumber ranging from 870 to 825 cm^{-1} .

Tensile Testing. For the mechanical testing, a molded sPS film was cut into a dog-bone shaped specimen, where the length and the width were 16.5 mm and 3 mm, respectively. To avoid breaking, the sample preparation was carried out at 110 °C, well above the glass transition temperature (T_g) of sPS. The tensile testing was performed at 130, 140, 160, 180, 204, and 218 °C by changing nominal strains from 10% to 50% at a strain rate of 5 mm/min using a tensile tester (AG-IS/TCE-N300 of Shimadzu and RSA3 of TA Instruments).

RESULTS AND DISCUSSION

Structural Analyses of an Amorphous Specimen and β Specimen. X-ray and FTIR analyses were conducted to verify the original microstructures of an amorphous specimen and β specimen (Figures S1–S4 in the Supporting Information). The WAXD results of the amorphous specimen clearly indicate that there were two broad peaks at the diffraction angles (2θ) of approximately 10.5° and 19.3°, which originated from amorphous regions reported in several papers (Figure S1).^{21,36} FTIR results of the amorphous specimen showed two clear peaks at the wavelengths of 905 and 841 cm^{-1} , which were exclusively attributed to amorphous regions (Figure S2). In the WAXD profile of the β specimen, plenty of peaks at $2\theta = 6.2^\circ$, 10.4°, 12.3°, 13.6°, 18.6°, 20.2°, 21.3°, and 23.9°, all due to β forms, were detected, while X-ray peaks caused by α forms were not detected (Figure S3). FTIR results of the β specimen also showed two large peaks at 911 and 858 cm^{-1} , which came from β forms in the β specimen (Figure S4). It should be noted that these two peaks appeared after subtracting the amorphous spectrum. Since there were no α peaks (902 and 851 cm^{-1}) detected through FTIR, it was concluded that our β specimen contained only β forms with some amounts of amorphous regions, however without α forms. It was therefore confirmed that β specimen and an amorphous specimen were successfully produced as intended.

β to α Transition Observed in β Specimen. Tensile testing of β specimen was performed at several temperatures to examine the effects of mechanical deformation on β forms. Figure 2 shows the stress–strain result of the β specimen up to 25% of nominal strain at 218 °C, which was almost close to the fracture point of sPS at this temperature. It was found that β specimen presented a

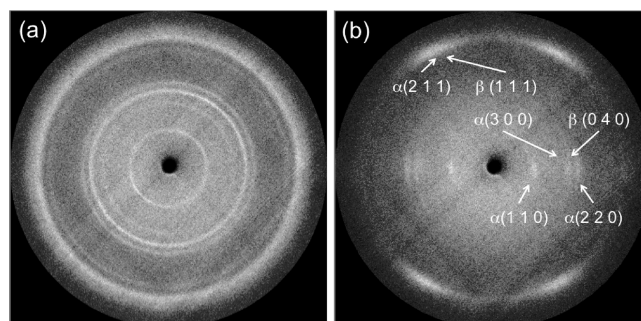


Figure 3. WAXS images observed at 218 °C: (a) 10% strain and (b) 20% strain.

clear yield point between 10% and 20%. Moreover, a clear upper yield point and a lower yield point were observed in β specimen.

Structural analyses of β specimen at each mechanical strain were conducted at 218 °C. Figure 3 shows the WAXS images of β specimen at nominal strains before yielding (10% strain) and after yielding (20% strain). For the materials stretched at lower than 10%, the X-ray peaks at the scattering angles of $2\theta = 6.2^\circ$, 10.4°, 12.3°, 13.6°, 18.6°, 20.2°, and 21.3° which were typical of β forms appeared. The results also indicated that the specimens were isotropic (the WAXS profile at 0% strain is in Figure S5a). The X-ray peak at $2\theta = 6.2^\circ$ resulted from (020) reflection, and other peaks at $2\theta = 10.4^\circ$, 12.3°, 13.6°, 18.6°, 20.2°, and 21.3° resulted from (110), (040), (130), (150), (111), and (041) reflections, respectively. The materials stretched to the strains of higher than 20% showed clear scattered spots instead of rings, indicating that the materials were strongly anisotropic with oriented α -form crystalline structures (the WAXS profile at 25% strain is in Figure S5b). The typical peaks of α form at the scattering angles of $2\theta = 6.8^\circ$, 11.7°, 13.6° and 20.2° came from (110), (300), (220), and (211) reflections, respectively. Thus, it was confirmed that there was a structural transition from isotropic to anisotropic phases between the strains of 10% and 20%. As was described above, the transition strain corresponded well with the strain of the yield point (measured between 10% and 20%) in the stress–strain curve of the samples. Figure 4 shows the X-ray diffraction profiles along the equatorial layer line of β specimen at each strain. Diffraction peak angles of $2\theta = 6.2^\circ$, 10.4°, 12.3°, 13.6°, 18.6°, 20.2°, and 21.3° were observed, which resulted from β forms, while no diffraction peaks from α forms were detected before yielding (10% strain). After yielding, on the other hand, not only β peaks but also diffraction peaks at $2\theta = 6.8^\circ$, 11.7° and 13.6°, all peculiar to α forms, were observed. From Figure 4, it was confirmed that the specimens before yielding predominantly contained β forms with amorphous phases, while the specimens after yielding contained α forms as well as β forms. The X-ray diffraction profiles of the β specimens after yielding (higher than 20% of strain) showed almost similar profiles regardless of mechanical strains.

Figure 5 shows FTIR spectra of the β specimen at each strain measured at 218 °C. The FTIR results matched quite well with the X-ray results, confirming that the structural transition of the β specimen occurred during the mechanical deformation. Figure 5 shows β peaks (911 and 858 cm^{-1}) in the β specimens stretched at lower than 10% of strain, while showing both β peaks (911 and 858 cm^{-1}) and α peaks (902 and 851 cm^{-1}) in the β specimens stretched at higher than 20% of strain. Also at above 20%, which was beyond the yield point of the β specimen, there were not any

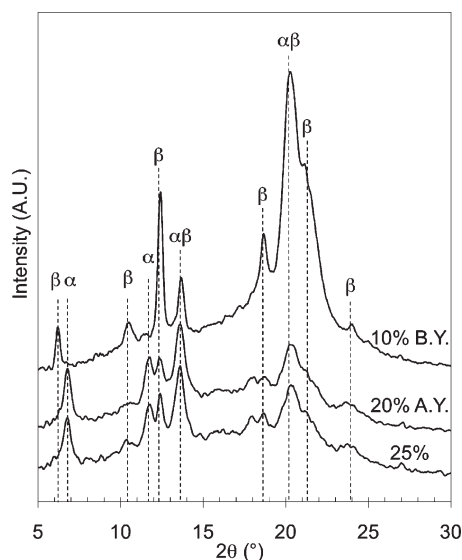


Figure 4. X-ray diffraction profiles at several strains. B.Y. and A.Y. represent “before yielding” and “after yielding”, respectively.

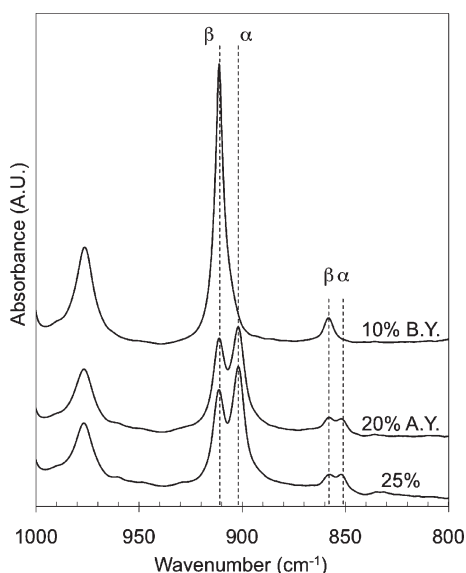


Figure 5. FTIR difference spectra at several strains. B.Y. and A.Y. stand for “before yielding” and “after yielding”, respectively.

significant changes observed in FTIR signals as well as in X-ray results, indicating that the structural transition was terminated by the strain of 20%. Hence, it is concluded that the clear solid to solid transition from β to α forms occurred during yielding. After yielding, the ratios of α forms, β forms, and amorphous regions remained constant irrespective of mechanical strains.

The actual ratios of α forms, β forms, and amorphous regions at each mechanical strain were calculated from the FTIR results by using eqs 1–3 (Figure 6). It was found that before yielding (before 10% strain) the ratios of α , β , and amorphous regions remained unchanged regardless of mechanical strains: the ratios of α , β , and amorphous regions remained approximately 0%, 61%, and 39%, respectively. After yielding (above 20% strain), it was found that α forms increased by $\sim 62\%$, while β forms and amorphous regions decreased by around 43% and 19%,

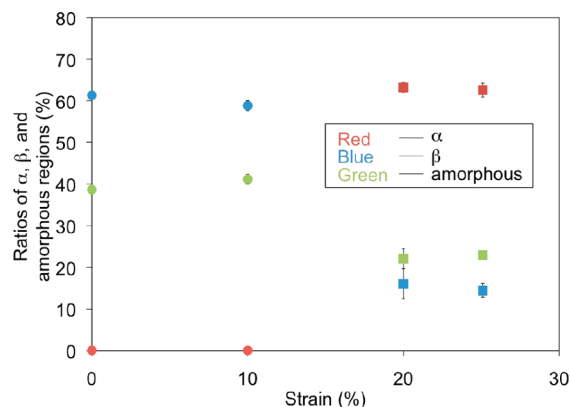


Figure 6. Ratios of α (red), β (blue), and amorphous (green) regions as a function of strain at 218 °C, before yielding (circles) and after yielding (squares).

respectively, where accordingly the degree of crystallinity increased. The ratios of each structure remained almost unchanged even when an additional mechanical strain was subsequently imposed on the specimens. It is therefore confirmed that the clear solid to solid transition (β to α transition) occurred right after the beginning of the yielding, and the transition was terminated right before the end of the yielding.

The reverse transition from α to β forms had already been reported by Sun et al.⁸ In their case, since α to β transition occurred at 260 °C, sPS should have started melting due to the melting temperature (270 °C), which was confirmed by DSC measurements. The transition may therefore be deemed as “a quasi-solid to solid transition” in their case. In our case, however, since the transition from β to α forms took place at 218 °C, which was well below the melting temperature of sPS, the transition can be well regarded as a solid to solid transition. This plain solid to solid transition has not been reported so far in sPS, and since ordinary industrial products chiefly contain α and β forms, the discovery may well be crucial to be used in industry.

β to α Transition at Different Temperatures. The structural transitions of β to α forms at 130, 140, 160, 180, and 204 °C were studied. The specimens could be drawn over 25% (Figure S6). Figure 7 and Figure S7 show the WAXS images of β specimen after yielding at different temperatures. Below 180 °C, two vague scattered X-ray spots of α form and mesomorphic α form were observed in the equator area. As temperature increased, the scattered spots became clearer and divided into three spots up to the temperature of 204 °C. Figure 8 and Figure S8 show the X-ray diffraction profiles along the equatorial layer line of β specimens at several strains and temperatures. Similar to the results of the X-ray diffraction at 218 °C, before yielding, only β peaks ($2\theta = 6.2^\circ, 10.4^\circ, 12.3^\circ, 13.6^\circ, 18.6^\circ, 20.2^\circ$, and 21.3°) were observed at each temperature. After yielding, not only β peaks but also a vague α peak ($2\theta = 6.8^\circ$) and other overlapping α peaks ($2\theta = 11.7^\circ$ and 13.6°) were observed in each sample at low temperature ($<180^\circ\text{C}$), while at high temperature ($>204^\circ\text{C}$), not only β peaks but also clear α peaks were observed (Figure 8). After yielding, X-ray diffraction profiles remained almost unchanged regardless of mechanical strains at any temperature. The broader α peaks observed at low temperatures ($<180^\circ\text{C}$) were most likely due to the overlap of β peaks with mesomorphic α forms. Figure 9 shows the X-ray diffraction profiles along the equatorial layer line at different temperatures

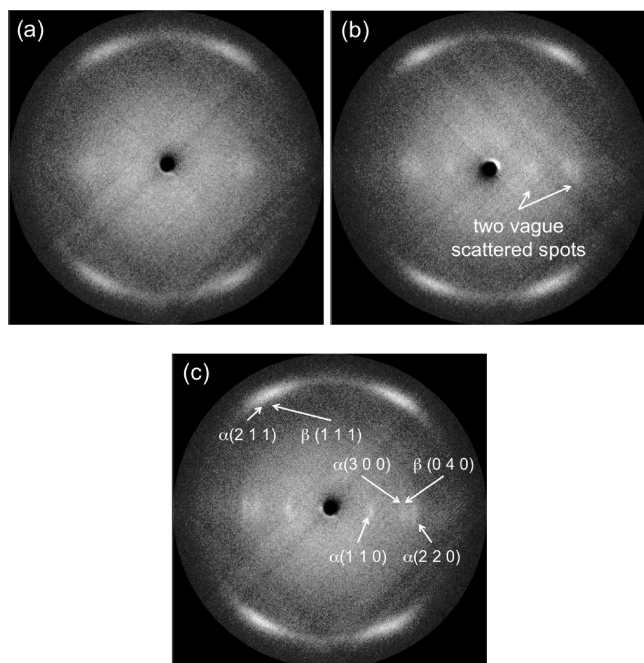


Figure 7. WAXS images of specimens after yielding at different temperatures of (a) 130, (b) 180, and (c) 204 °C.

after yielding, where the α peaks became more pronounced as temperature increased. These results showed that at low temperature (<180 °C) the specimen contained principally mesomorphic α forms with small amount of perfect α forms, whereas above 204 °C, the perfect α forms increased with decrease in mesomorphic α forms until the specimens contained mainly α forms at 218 °C.

Figure 10 and Figure S9 show the results of FTIR spectra observed at 130, 140, 160, 180, and 204 °C, stretched at the strains of 10%, 20%, 30%, 40%, and 50%. Similar to the X-ray results, it was revealed from the FTIR results that before yielding only β peaks (911 and 858 cm^{-1}) existed, and after yielding, not only β peaks but also α peaks (902 and 851 cm^{-1}) were observed in each sample at different temperatures. Also after yielding, the peaks of the FTIR signals remained almost unchanged by mechanical strains at each temperature. It was therefore found that, from the results of X-ray analysis and FTIR analysis, β to α transition occurred during yielding at all tested temperatures. The ratios of α , β , and amorphous regions were calculated from FTIR results at different temperatures (Figure 11 and Figure S10). The results also demonstrated that the ratios of α , β , and amorphous regions remained almost unchanged before yielding. During yielding, α forms increased while β forms and amorphous regions decreased. After yielding, the ratios stayed almost constant, whereas the degree of crystallinity increased as temperature increased. It was therefore confirmed that the β to α transition occurred during yielding for all tested temperatures and that the ratios of α , β , and amorphous regions were independent of mechanical strains after yielding.

It was concluded that there were no α forms at the initial stage of stretching, which lasted up to the beginning of the yielding.

DISCUSSION

There have been several reports that dealt with the effects of the mobility of polymer chains on the structure and the structural

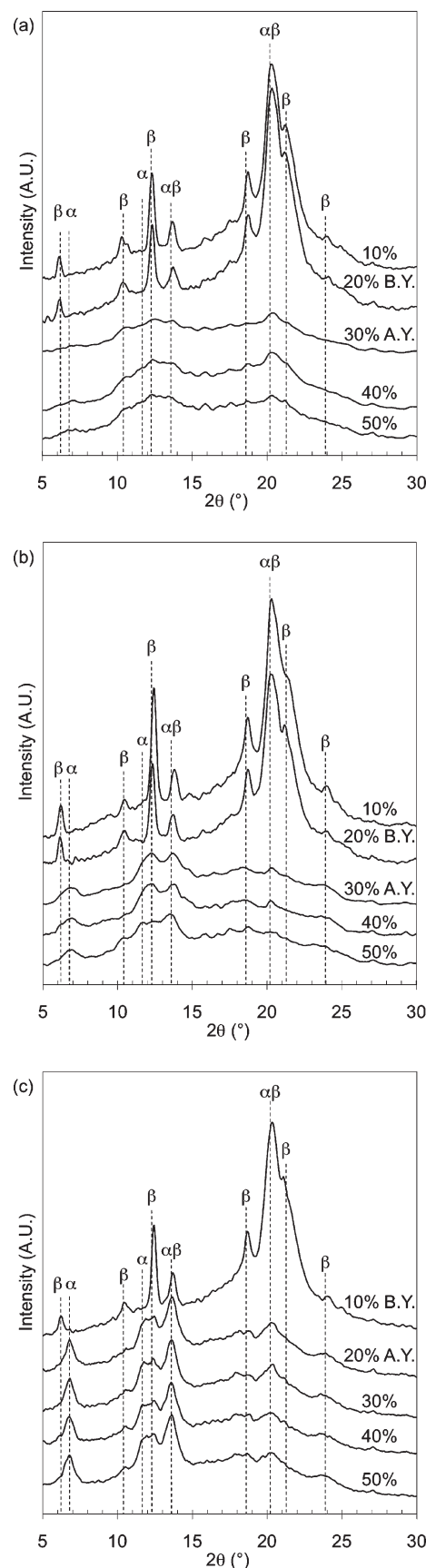


Figure 8. X-ray diffraction profiles by changing strains at different temperatures of (a) 130, (b) 180, and (c) 204 °C. B.Y. and A.Y. stand for “before yielding” and “after yielding”, respectively.

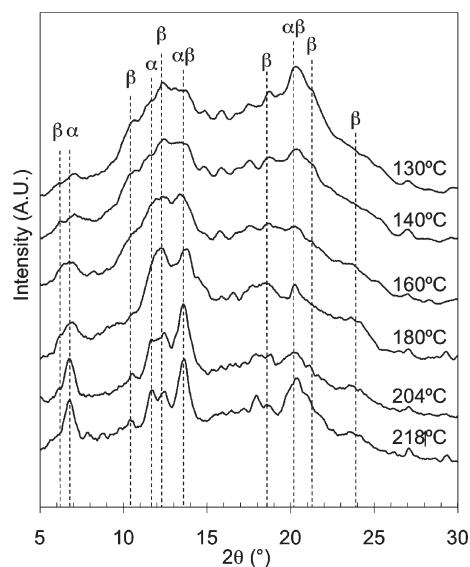


Figure 9. X-ray diffraction profiles at different temperatures after yielding.

transitions of PS and sPS.^{7,19,37,38} From the researches, it was found that the mobility of the molecular chains had strong effects on the structural transitions in crystalline sPS. For example, Gowd et al. studied a sPS solvent complex and reported that higher content of solvent exhibited lower transition temperature in the structural transition from δ to γ forms.³⁷ They considered that solvent in amorphous phases increased the mobility of amorphous polymer chains, which eventually reduced the transition temperature. As for the structural transition from γ to β forms, Rizzo et al. concluded that the lower transition temperature was due to the higher amount of solvent, which brought about the plasticizing effect in amorphous phases.^{7,19} From these researches, it was suggested that the mobility of molecular chains was a very important factor affecting the structural transitions in crystalline sPS.

A structural transition from α to β forms was reported by Sun et al. As was mentioned above, they reported that α to β transition occurred when α form was annealed at 260 °C with the compression pressure of 118 kPa.⁸ The melting temperature of sPS was around 270 °C, which was only 10 °C higher than the annealing temperature, where some parts of α forms and amorphous regions started to melt and transform into β forms, confirmed by the broad peak of the enthalpy of fusion at the melting temperature in DSC. The reported α to β transition can thus be referred to as a “quasi-solid to solid transition” through a “liquid” state. The important thing here was that the transition could only be realized at very high temperature with high mobility of molecular chains.

In our experiments, the reverse transition from β to α forms was found at significantly low temperature, which can be well referred to as an actual solid to solid transition. The low temperature required for the transition indicates that β to α transition would not possibly demand high mobility of polymer chains, which is unlike the above-mentioned α to β transition. It was reported by De Rosa that an oriented fiber sample of sPS in the α form was obtained by stretching compression-molded specimens at 160 °C, which may have contained β form.¹⁰ Sun et al. introduced an interesting sPS behavior resulted from the difference in the formation processes of two different crystalline structures: α forms could be easily produced in partially solidified

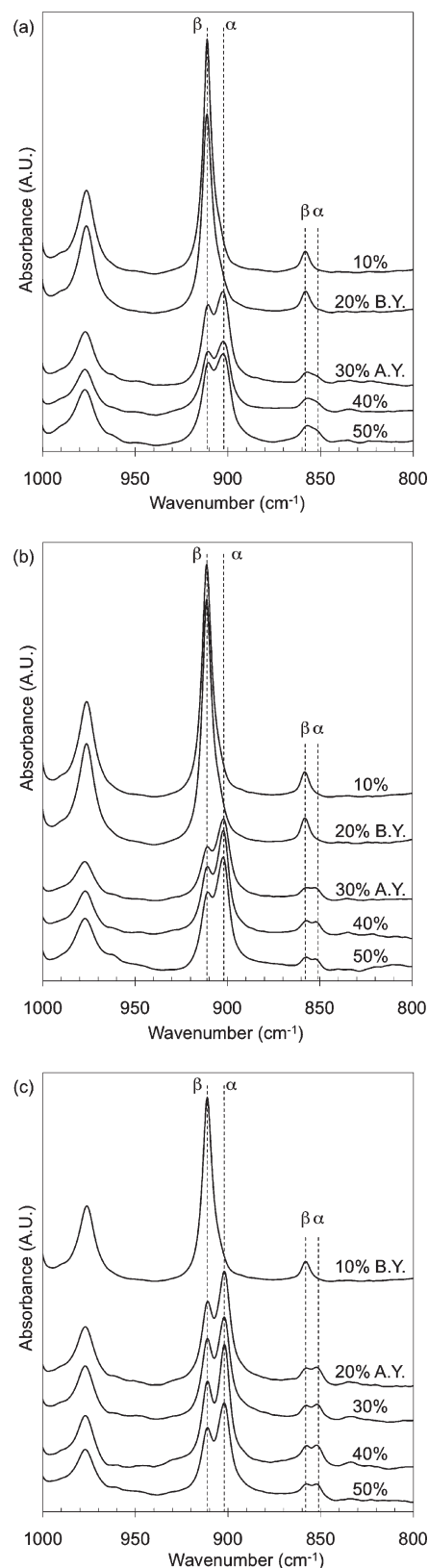


Figure 10. FTIR difference spectra as a function of strain at temperatures of (a) 130, (b) 180, and (c) 204 °C. B.Y. and A.Y. stand for “before yielding” and “after yielding”, respectively.

sPS with low mobility of polymer chains in semicrystalline structures,³⁹ whereas β forms could be produced in an either

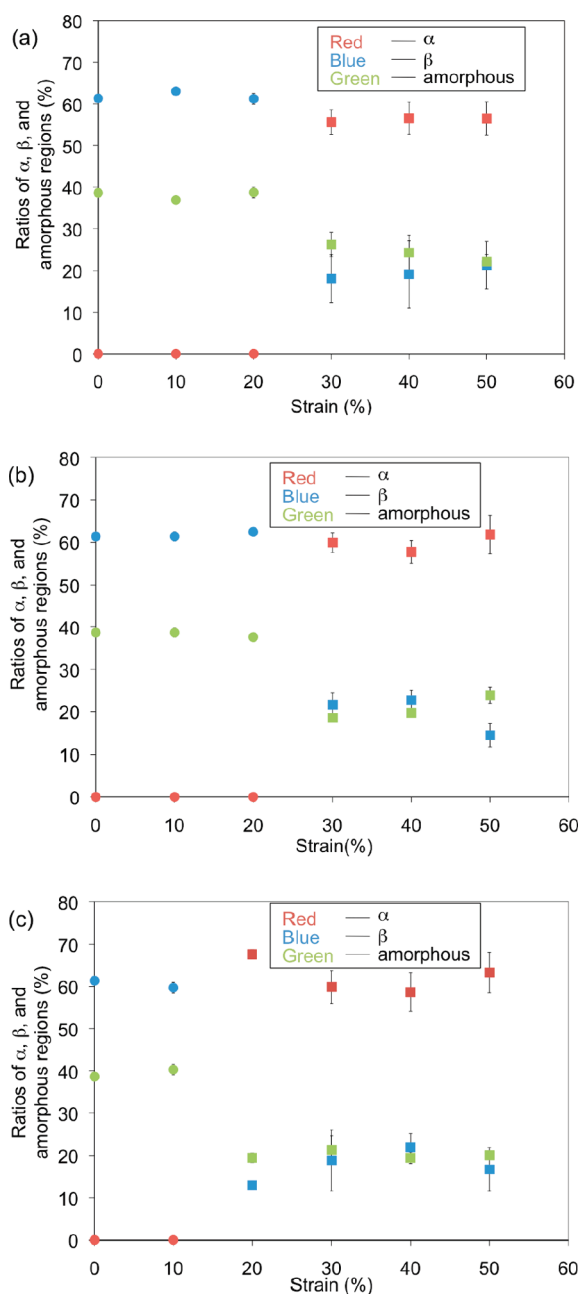


Figure 11. Ratios of α (red), β (blue), and amorphous (green) regions as a function of strain at temperatures of (a) 130, (b) 180, and (c) 204 °C, before yielding (circles) and after yielding (squares).

molten or dissolved state of sPS with higher mobility of polymer chains. Instead, it was also reported that α form was dominant in cold crystallization which was usually carried out at lower temperature with lower mobility of polymer chains (in a solid state), than ordinary melt crystallization. Therefore, we concluded that the β to α transition could be accomplished in a solid state of sPS and that β to α transition was indeed a solid to solid transition. In the same manner, it was also concluded that α to β transition could occur in a liquid state of sPS, since β form could be produced in a liquid state of sPS.

Another intriguing result in our experiments was that the mechanical stretching could cause the β to α transition, while it was reported that the mechanical compression induced the α to

β transition.⁸ It is known that the densities of α forms, β forms, and amorphous regions are 1.03, 1.08, and 1.06 g/cm³, respectively. The density of β forms is the largest among them, while the density of α form is the smallest. From our experimental results, it was found that, when mechanical strain was applied to β specimens, the specimens became less dense for β forms to transform into α forms in order to be more structurally stable. Meanwhile, since the density became lower during the transition from β to α forms, it can be readily stated that the volume of β forms increased to become α forms. Considering every density of the sPS structures, the density of amorphous regions lies in between that of β forms (higher) and that of α forms (lower). The β forms may therefore first transform into amorphous regions followed by the transition from amorphous regions to α forms in order to finally complete the overall β to α transition.

CONCLUSION

In this research, a solid to solid transition from β to α forms in sPS induced by mechanical stretching was first discovered and discussed. From the X-ray and the FTIR results, it was revealed that this transition occurred during yielding at a temperature range of 130–218 °C. The difference between the α to β transition and the β to α transition was discussed. For the α to β transition, high mobility of molecular chains was necessary to induce the transition, revealing that the α to β transition induced by compression was a quasi-solid to solid transition observed at around the melting temperature of sPS. The reverse transition from β to α forms, on the other hand, was found to be a solid to solid transition, occurring at much lower temperature (well below the melting temperature of sPS) with lower mobility of molecular chains. The difference between these two transitions may possibly be due to the difference in the crystallization behavior of α forms and β forms: α forms can be produced in solidified sPS with lower mobility of molecular chains, while β forms can be produced in an either molten or dissolved state of sPS. The directions of mechanical deformations, such as compression and tension, were found to be intimately related with the types of the transitions: the process of compression induced α to β transition with volume contraction (higher in density), while the process of mechanical tension induced β to α transition with volume expansion (lower in density).

The structural transitions between these two major crystalline structures, α forms and β forms, can be effectively utilized in industry owing to the readily accessible crystalline structures produced by a concise molding process.

ASSOCIATED CONTENT

Supporting Information. FTIR results, X-ray results, and stress–strain results. This material is available free of charge via the Internet at <http://pubs.acs.org>.

AUTHOR INFORMATION

Corresponding Author

*Tel +81-45-566-1604; Fax +81-45-566-1495; e-mail hotta@mech.keio.ac.jp.

ACKNOWLEDGMENT

This work was supported in part by a Grant-in-Aid for the Global Center of Excellence Program for the “Center for

Education and Research of Symbiotic, Safe and Secure System Design” from the Ministry of Education, Culture, Sport, and Technology in Japan (A.H.), a Grant-in-Aid for Exploratory Research from the Japan Society for the Promotion of Science (JSPS: “KAKENHI”) (No. 21656167 to A.H.), a Grant-in-Aid for Scientific Research (S) (No. 21226006 to A.H.), and a Grant-in-Aid for Scientific Research on Innovative Areas (No. 22110516 to A.H.). Idemitsu Kosan Co., Japan, was greatly appreciated for the supply of SPS specimens.

REFERENCES

- (1) Natta, G.; Pino, P.; Corradini, P.; Danusso, F.; Mantica, E.; Mazzanti, G.; Moraglio, G. *J. Am. Chem. Soc.* **1955**, *77* (6), 1708–1710.
- (2) Ishihara, N.; Seimiya, T.; Kuramoto, M.; Uoi, M. *Macromolecules* **1986**, *19* (9), 2464–2465.
- (3) Gowd, E. B.; Tashiro, K.; Ramesh, C. *Prog. Polym. Sci.* **2009**, *34* (3), 280–315.
- (4) Woo, E. M.; Sun, Y. S.; Yang, C. P. *Prog. Polym. Sci.* **2001**, *26* (6), 945–983.
- (5) Yee-Chan, C. K.; Scogna, R. C.; Register, R. A. *Elevation of the Glass Transition Temperature in Flexible-Chain Semicrystalline Polymers*; Wiley Subscription Services, Inc.: New York, 2007; Vol. 45, pp 1198–1204.
- (6) De Rosa, C.; Ruiz de Ballesteros, O.; Di Gennaro, M.; Auriemma, F. *Polymer* **2003**, *44* (6), 1861–1870.
- (7) Rizzo, P.; Alburnia, A. R.; Guerra, G. *Polymer* **2005**, *46* (23), 9549–9554.
- (8) Sun, Z.; Morgan, R. J.; Lewis, D. N. *Polymer* **1992**, *33* (3), 660–661.
- (9) Sun, Y. S.; Woo, E. M. *Macromol. Chem. Phys.* **2001**, *202* (9), 1557–1568.
- (10) De Rosa, C. *Macromolecules* **1996**, *29* (26), 8460–8465.
- (11) Greis, O.; Xu, Y.; Asano, T.; Petermann, J. *Polymer* **1989**, *30* (4), 590–594.
- (12) De Rosa, C.; Guerra, G.; Petraccone, V.; Pirozzi, B. *Macromolecules* **1997**, *30* (14), 4147–4152.
- (13) Manfredi, C.; Rosa, C. D.; Guerra, G.; Rapacciuolo, M.; Auriemma, F.; Corradini, P. *Macromol. Chem. Phys.* **1995**, *196* (9), 2795–2808.
- (14) De Rosa, C.; Rapacciuolo, M.; Guerra, G.; Petraccone, V.; Corradini, P. *Polymer* **1992**, *33* (7), 1423–1428.
- (15) Chatani, Y.; Shimane, Y.; Ijitsu, T.; Yukinari, T. *Polymer* **1993**, *34* (8), 1625–1629.
- (16) Auriemma, F.; Petraccone, V.; Dal Poggetto, F.; De Rosa, C.; Guerra, G.; Manfredi, C.; Corradini, P. *Macromolecules* **1993**, *26* (15), 3772–3777.
- (17) Rastogi, S.; Goossens, J. G. P.; Lemstra, P. J. *Macromolecules* **1998**, *31* (9), 2983–2998.
- (18) Yan, R. J.; Ajji, A.; Shinozaki, D. M.; Dumoulin, M. M. *Polymer* **2000**, *41* (3), 1077–1086.
- (19) Gowd, E. B.; Tashiro, K. *Macromolecules* **2007**, *40* (15), 5366–5371.
- (20) Gowd, E. B.; Nair, S. S.; Ramesh, C. *Macromolecules* **2002**, *35* (22), 8509–8514.
- (21) Guerra, G.; Vitagliano, V. M.; De Rosa, C.; Petraccone, V.; Corradini, P. *Macromolecules* **1990**, *23* (5), 1539–1544.
- (22) Gowd, E. B.; Nair, S. S.; Ramesh, C.; Tashiro, K. *Macromolecules* **2003**, *36* (19), 7388–7397.
- (23) Su, C. H.; Jeng, U.; Chen, S. H.; Cheng, C. Y.; Lee, J. J.; Lai, Y. H.; Su, W. C.; Tsai, J. C.; Su, A. C. *Macromolecules* **2009**, *42* (12), 4200–4207.
- (24) Su, C. H.; Chen, S. H.; Su, A. C.; Tsai, J. C. *J. Polym. Res.* **2004**, *11* (4), 293–298.
- (25) Lin, R. H.; Woo, E. M. *Polymer* **2000**, *41* (1), 121–131.
- (26) Ho, R.-M.; Lin, C.-P.; Hsieh, P.-Y.; Chung, T.-M.; Tsai, H.-Y. *Macromolecules* **2001**, *34* (19), 6727–6736.
- (27) Ho, R.-M.; Lin, C.-P.; Tsai, H.-Y.; Woo, E.-M. *Macromolecules* **2000**, *33* (17), 6517–6526.
- (28) Decandia, F.; Ruvolo, A.; Vittoria, V. *Makromol. Chem., Rapid Commun.* **1991**, *12* (5), 295–299.
- (29) Gowd, E. B.; Shibayama, N.; Tashiro, K. *Macromolecules* **2006**, *39* (24), 8412–8418.
- (30) Gowd, E. B.; Shibayama, N.; Tashiro, K. *Macromolecules* **2008**, *41* (7), 2541–2547.
- (31) Gowd, E. B.; Shibayama, N.; Tashiro, K. *Macromolecules* **2007**, *40* (17), 6291–6295.
- (32) Musto, P.; Tavone, S.; Guerra, G.; Rosa, C. D. *J. Polym. Sci., Part B: Polym. Phys.* **1997**, *35* (7), 1055–1066.
- (33) Wu, H.; Wang, W.; Yang, H.; Su, Z. *Macromolecules* **2007**, *40* (12), 4244–4249.
- (34) Wu, S.-C.; Chang, F.-C. *Polymer* **2004**, *45* (3), 733–738.
- (35) Wu, H.-D.; Wu, S.-C.; Wu, I. D.; Chang, F.-C. *Polymer* **2001**, *42* (10), 4719–4725.
- (36) Sun, Y. S.; Woo, E. M. *Polymer* **2001**, *42* (5), 2241–2245.
- (37) Gowd, E. B.; Tashiro, K.; Ramesh, C. *Macromolecules* **2008**, *41* (24), 9814–9818.
- (38) Baeurle, S. A.; Hotta, A.; Gusev, A. A. *Polymer* **2005**, *46* (12), 4344–4354.
- (39) Sun, Y. S.; Woo, E. M. *Macromolecules* **1999**, *32* (23), 7836–7844.